Optimizing the internal design of a miniaturized fluidic oscillator for active flow control over a scaled NACA-4412

Guillermo Lopez Quesada, Ahmad Batikh, Stéphane Orieux, Nicolas Mazellier, Lucien Baldas

56th 3AF International Conference on Applied Aerodynamics
28 – 30 March 2022, Toulouse - France

FP110-AERO2022-lopezquesada

Optimizing the internal design of a miniaturized fluidic oscillator for active flow control over a scaled NACA-4412

LOPEZ QUESADA Guillermo[(1)], BATIKH Ahmad[(1) (2)], ORIEUX Stéphane[(1)], BALDAS Lucien[(1)], MAZELLIER Nicolas[(3)]

[(1)] *Institut Clément Ader (ICA), Université de Toulouse, CNRS, INSA, ISAE-SUPAERO, Mines Albi, UPS, Toulouse France, Email: glopezqu@insa-toulouse.fr*

[(2)] *ICAM-Toulouse, 75 avenue de Grande-Bretagne, 31076 TOULOUSE Cedex 3, France*

[(3)] *University of Orléans, INSA-CVL, PRISME, EA 4229, 45072 Orléans, France*

ABSTRACT

The detachment of the boundary layer over the wing of an aircraft and its detrimental effects during the critical phases of the flight (mainly take-off and landing) has been extensively studied [1]. Controlling the separation of the boundary layer decreases the energy consumption (and consequently CO2 emissions) while also improving the maneuvering capability, safety, and durability of the aircraft by suppressing instabilities. Active flow control by means of pulsed jets along the span of the wing can be used to compensate for the momentum deficit in the boundary layer to delay its detachment from the airfoil [2]. However, implementing active flow control devices leading to a net gain in the energy balance remains an open issue which the CleanSky PERSEUS project attempts to address. The focus of the presented work is on the design of the Pulsed Jet Actuators and the optimization of their internal geometry to provide a targeted performance over a scaled NACA-4412 airfoil.

1. INTRODUCTION

In order to control the separation of the boundary layer with active flow control techniques, a variety of actuators can be found in the literature [3]. Among these, fluidic oscillators have been in a rising trend in the recent years because their oscillations are completely self-induced and self-sustained and only depend on the internal fluid dynamics, without any moving part, which is positive in terms of reliability and robustness.

In the ongoing Cleansky PERSEUS project, the goal is to design, fabricate and implement different assemblies of fluidic oscillators that will permit an active control of the turbulent flow separation over a scaled NACA-4412 airfoil (length of wingspan 110 cm, chord 30 cm). In the present work, the focus is on the internal design of the fluidic oscillators taking into account the fabrication constraints of the actuators, the physical constraints linked to the scaled airfoil and the targeted performances for the future tests in the wind tunnel.

An experimental characterization of the scaled NACA-4412 airfoil has already been conducted in the wind tunnel of the PRISME laboratory (Orléans, France); along with numerical simulations and a sensitivity analysis to determine the most sensible location and injection angle of the PJAs to apply for the active flow control [4]. The characterization was provided for a free stream velocity of the wind tunnel U_∞ =30-50 m/s. The sensitivity analysis shows that in order to improve the aerodynamic performances (i.e. lift-to-drag ratio), the PJAs should be located close to the leading edge and the momentum should be injected tangentially to the boundary layer.

Therefore, the plan is to design and manufacture different PJAs covering 55% of the wingspan length (60 cm length of the PJAs body), with the outlets at different positions from the leading edge (i.e. 5% - 15% of the chord length), and having the direction of the outlets as tangentially as possible to the airfoil surface. As a result, the PJAs will 3D printed in one piece and integrated into the airfoil as shown in Fig. 1-a and Fig. 1-b. The objective being to allow flow control along the span of the wing, a large assembly of oscillators is required. If the oscillators were left independent from each other, their oscillatory frequencies could vary or not be in phase due to manufacturing imperfections or variations in the operating conditions. However, the

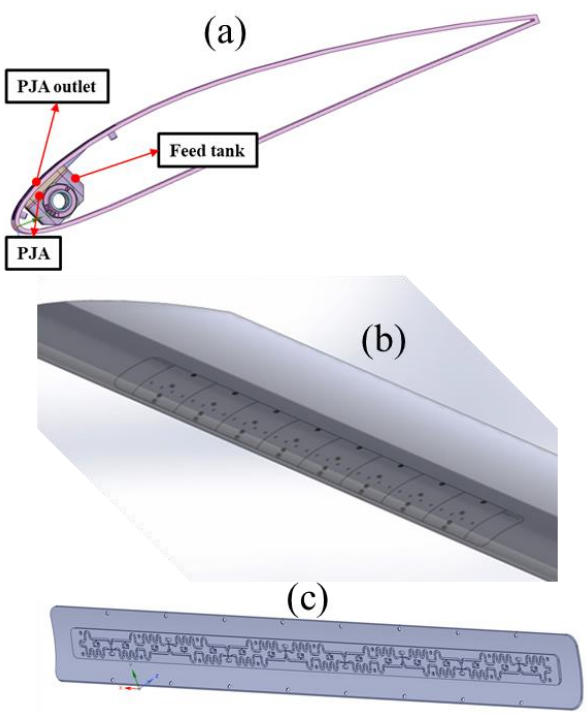

Figure 1: (a) interior and (b) exterior view of PJAs implemented in an airfoil and (c) internal design of the interconnected fluidic oscillators.

proposed design allows for a self-induced synchronization of the assembly by interconnecting the feedback loops of the different oscillators (Fig. 1-c). A total of 6 oscillators will be included in the 60 cm length along the span of the wing allocated for the PJAs, providing 12 outlets with a separation of 44 mm between the pulsated jets outlets.

For the purpose of evaluating and comparing the efficiency of a jet injection for the separation control, three dimensionless numbers are typically use: the injection momentum coefficient C_μ (Eq. 1), the velocity ratio V_R (Eq. 2) and the injection frequency F^+ (Eq. 3)

$$C_\mu = \frac{\overline{m_{out} V_{out}}}{\frac{1}{2}\rho U_\infty^2 L\omega} \qquad (1)$$

$$V_R = \frac{V_{max}}{U_\infty} \qquad (2)$$

$$F^+ = \frac{fL}{U_\infty} \qquad (3)$$

Where m_{out} is the injected mass flow rate by the PJAs, V_{out} is the velocity at the outlets of the PJAs, ρ is the density of the injected fluid, L is the flow characteristic length (typically the chord), ω is the span width of the controlled flow, V_{max} the maximum velocity at the outlets, f the oscillation frequency and U_∞ the free stream velocity around the airfoil.

Several works have studied the optimal values of these parameters on ramp or hump flows [5-9]. For C_μ, large discrepancies have been found by different groups which could be explained by the large difference between the studied configurations. However, in most cases, the optimal values found for V_R are between 2 and 3, and the optimal F^+ is between 1 and 3. Consequently, the targeted performance of the PJAs to be design should be close to these values of V_R and F^+, which for the particular case on the scaled NACA-4412 airfoil considered (length 1 m, chord 0.3 m and free stream velocity of the wind tunnel U_∞ =30-50 m/s) result in maximum outlet velocities V_{max} =60-150 m/s and oscillatory frequency in the range f =100-500 Hz.

The present paper shows first the working principle of the fluidic oscillator, its basic design and the methodology followed for the numerical simulations. Next, an initial design is proposed and evaluated, highlighting an unexpected behaviour of the oscillator differing from the anticipated performance. Then, a modified design is proposed with significant changes in the geometry correcting the deviation from the expected operation found on the initial design. In addition, a prototype fabricated following this modified design is characterized with hot wire anemometry to compare with the numerical investigation. Finally a conclusion is proposed and future steps are discussed.

2. WORKING PRINCIPLE

The Pulsed Jet Actuators introduced in this work are based on bi-stable relaxation fluidic oscillators [10] with some modifications in order to make them suitable for their integration in the NACA4412 airfoil. These new PJAs (Fig. 2) consist of one inlet nozzle connected to a switching zone that is divided by a splitter in two branches (S1 and S2), each of them leading towards a feedback loop (F1 and F2). These feedback loops reconnect to the switching zone through their respective control ports (C1 and C2). At the beginning of each

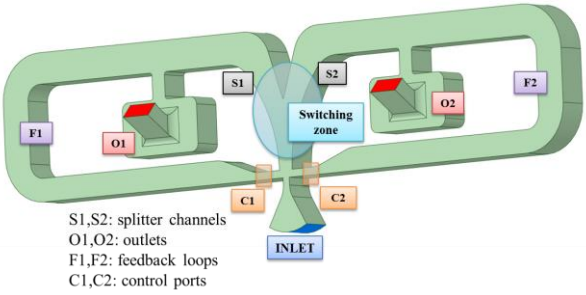

Figure 2: geometry of a single fluidic oscillator.

feedback loop an elbow connects with a reservoir and the outlet channels (O1 and O2).

The oscillatory behavior of the actuator is provided by the feedback loop geometry and the control ports connected to the switching zone. Considering for example an initial flow from the inlet nozzle attached, thanks to the Coanda effect, to the branch S1, part of the flow would exit from the actuator through the outlet O1 while the rest of the flow would run along the feedback loop F1 and its corresponding control port C1, increasing the pressure in this loop with a compression wave propagating roughly at the speed of sound. When this pressure wave reaches C1, it is reflected back and generates a pressure increase at the connection between F1 and S1. The same phenomena occur but with expansion waves on the other side of the oscillator. Thus, the pressure imbalance between S1 and S2 together with pressure imbalance between C1 (control port with flow, higher pressure) and C2 (control port without flow, lower pressure), results in the switching of the flow stream from S1 towards S2. Then this process is repeated in the same way for the opposite feedback loop F2 and control port C2, providing the oscillatory change of the flow stream from S1 to S2 and effectively generating pulsating jets at the outlets O1 and O2.

Following this, the main control parameter for the frequency f of oscillation is typically the length L_{fb} of the feedback loop as shown in Eq. 4 [10], where C_0 is the speed of the pressure wave propagation, typically the speed of sound, which travels back and forth each of the two feedback loops during one period.

$$f = \frac{C_0}{4 \times L_{fb}} \qquad (4)$$

Considering the targeted frequency of the PJAs should be f =100-500 Hz (corresponding to F^+ =1-3), the range of the feedback loop length is L_{fb} =170-850 mm. However, given the spatial constraints due to the limited separation between oscillators of only 44 mm, the classic simple feedback loop design must be changed and increased in complexity.

3. METHODOLOGY

The numerical investigation has been performed with ANSYS Fluent using the coupled solver, the realizable k-ε turbulent model and a second order upwind spatial discretization scheme. A preliminary validation of the methodology was done on a first simple model to check the numerical dependence on the mesh quality and time step size of the unsteady simulation. The 3D model of 2 synchronized oscillators shown in Fig. 3-a was meshed with 3 different mesh sizes resulting in approximately $6.5 \cdot 10^5$, $1.5 \cdot 10^6$ and $7 \cdot 10^6$ elements. Three time step

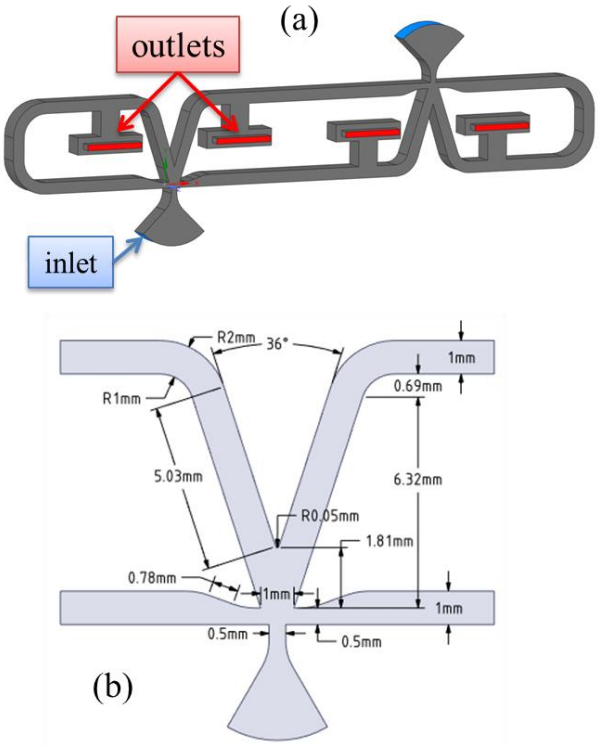

Figure 3: (a) 3D model of 2 synchronized oscillators and (b) detailed view of the switching zone.

Table 1: Comparison of the frequency calculated for different mesh densities and time step sizes.

		Time step size (s)			
		1.00E-05	1.00E-06	1.00E-07	
mesh density (million elements)	0.65	3225	3037	3014	f (Hz)
		12.82%	7.41%	6.72%	(%)
	1.50	2908	2877	2885	f (Hz)
		3.29%	2.25%	2.53%	(%)
	3.00	2880	2843	2812	f (Hz)
		2.34%	1.09%	-	(%)

sizes were used 10^{-5} s, 10^{-6} s and 10^{-7} s. A detail of the switching zone is shown in Fig. 3-b. The feedback loop length is L_{fb} =30mm and the outlet sections are 1x5 mm^2. The inlet total pressure is 3 bar while the outlets are considered as pressure outlets kept at 1 bar. With the given geometry, the frequency of oscillation calculated from Eq.4 should be around 2833 Hz.

In Table 1, the oscillation frequency obtained for the 9 different configurations in terms of mesh density and time step size are shown. The relative difference between each of the simulations compared to the most detailed case ($7 \cdot 10^6$ elements and 10^{-7} s) is also displayed. The results in terms of mesh density, for $1.5 \cdot 10^6$ and $3 \cdot 10^6$ elements show a relative difference between 1.09% and 3.29%, with the error increasing with the time step size. On the other hand, the coarser mesh ($6.5 \cdot 10^5$ elements) provide a much bigger

difference, with the oscillation frequency being 6.72% to 12.82% larger than the reference case when the time step size is increased from 10^{-7} s to 10^{-5} s. Following this sensitivity analysis in terms of the mesh density and the time step size, the configuration with $1.5 \cdot 10^{6}$ elements and a time step size of 10^{-5} s provides a good compromise between computing time and accuracy of results. With this configuration the deviation from the reference case is only 3.29% while the computing time is greatly reduce. With this particular mesh density, the 1st inflation layer next to the wall is smaller than $4 \cdot 10^{-5}$ m resulting in a maximum value of y^+ around 37 to resolve the turbulent flow with the standard wall function treatment. Therefore, the numerical investigation provided in the following sections will be using similar mesh characteristics and a time step size of 10^{-5} s. Also, at least 2 oscillators will be simulated in order to check a proper synchronization between the jets at the outlets.

4. INITIAL DESIGN

The initial design is shown in Fig. 4-a where the geometry of the switching zone is identical to the one in Fig. 3-b, but the simple feedback loop geometry is replaced by a longer feedback loop with several serpentines in order to accommodate a large feedback loop length within the 44mm of separation between oscillators. The total feedback loop length is L_{fb} =190 mm, with a width of 1mm. The depth of the oscillators is 2 mm while the outlets section is 1x2 mm^2.

The numerical results for the average velocity profiles at the outlet are shown in Fig. 4-b, with the oscillating jet displaying velocities of between 70 m/s and 180 m/s and a frequency of oscillation f =743 Hz. The maximum velocity around 180 m/s is slightly over the targeted V_{max} of 60-150 m/s, but this is not a big concern since the outlet section can be increased to reduce the overall velocity at the outlets. It should be noted that the after an initial transitory state for the first oscillation, a stable regime is reached with a proper synchronization between the 2 oscillators However, the frequency of oscillation f =743 Hz is significantly larger than the expected one (Eq.4) of 450 Hz. Therefore the internal flow of the fluidic oscillators is analyzed in Fig. 4-c by observing the velocity contours in the middle plane of the switching zone at four different times during one oscillation period (i.e. each quarter of the period). It is evident then, that the fluidic oscillators were not working as intended since the flow was flapping around the splitter walls instead of switching completely from one branch to the other.

In a first attempt to address this issue, the inlet total pressure was increased up to 5 bar but the oscillatory frequency still remained around 750 Hz. It seems that due to the increased complexity in the feedback loop combined with its small size (1x1 mm^2 cross section) generates a rather high resistance to the flow. This causes the flow to be mostly directed towards the outlet reservoirs instead of filling the feedback loops, failing to generate the required pressure waves for a complete switch of the jet from one branch to the other.

Therefore, for the following iteration of the numerical study of the PJAs, the width and depth of the feedback loop was increased and the complexity of the feedback loop was reduced. This however, limits the length of the feedback loop, making it difficult to reach the targeted oscillatory frequency. Additionally, in order to facilitate the Coanda effect and help attaching the jet to the walls opposite to the splitter, the walls in the switching zone were made slightly rounded.

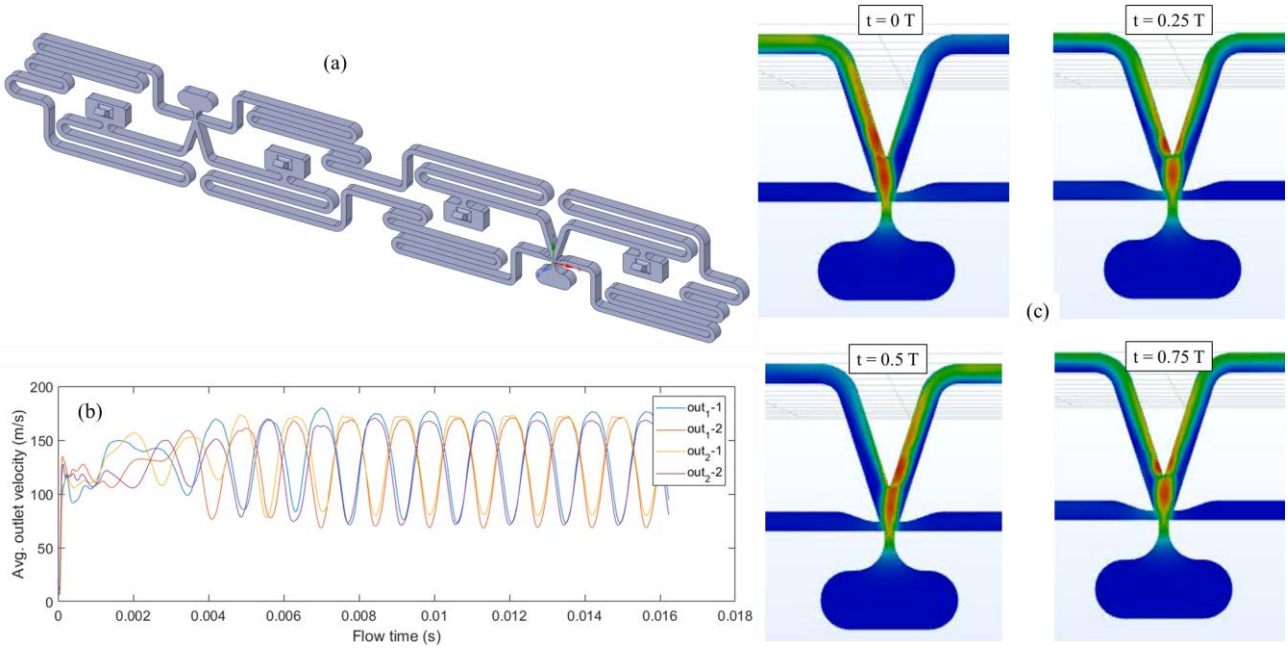

Figure 4: (a) 3D model of 2 synchronized oscillators of the initial design, (b) average velocity at each of the four outlets and (c) velocity contours in the switching zone at four different times during one period of the oscillation.

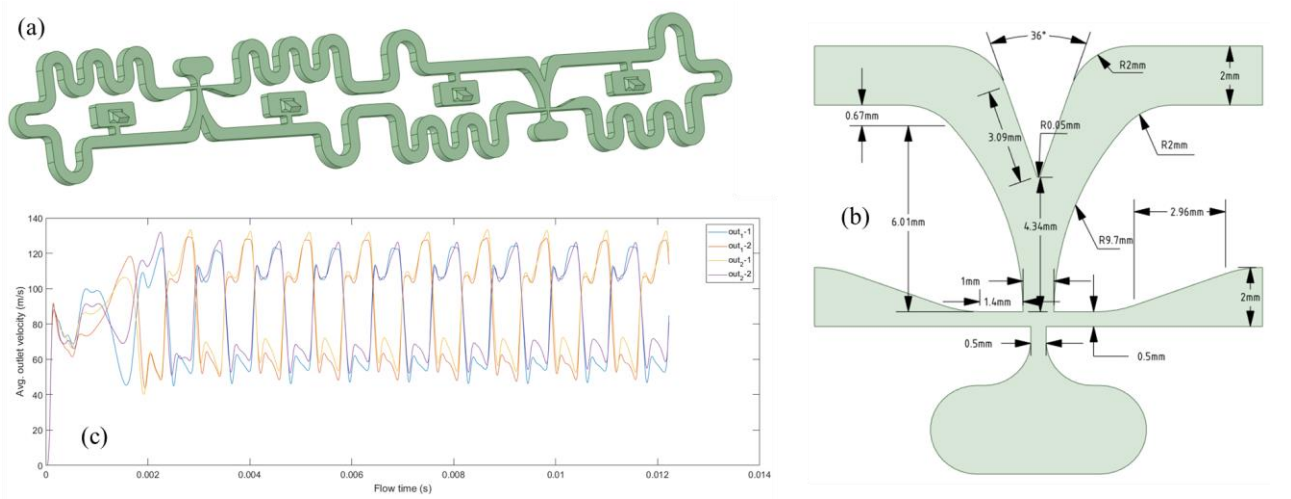

Figure 5: (a) 3D model of 2 synchronized oscillators of the modified design, (b) detailed view of the switching zone geometry and (c) average velocity at each of the four outlets.

5. MODIFIED DESIGN

The modified design is shown in Fig. 5-a with a detailed view of the adjusted switching zone in Fig. 5-b. The feedback loop length is set to 100 mm. This should provide a slightly larger oscillatory frequency than initially targeted (expected frequency of 850 Hz), but with the given constraints in terms of size, the focus is now to have a fluidic oscillator with a proper switching. The inlet total pressure is set to 3 bar while the outlets are kept at atmospheric pressure.

The average velocity at the outlets is shown in Fig. 5-c, with an oscillatory frequency of 817Hz and values going from around 45 m/s to 125 m/s. It can also be observed that the after an initial transitory state for the first oscillation, a stable regime is reached with a proper synchronization between the 2 oscillators. The flow in the switching zone is shown in Fig. 6 at different times revealing that the switching is indeed complete in this case from one branch to the other. Additionally, it can be observed how a recirculation bubble is generated between the jet and the splitter when the jet is completely attached to the branch walls. This could be a potential phenomenon to exploit in order to delay the switching of the jet and decrease the oscillatory frequency of the PJAs even while keeping the same feedback loop geometry.

6. EXPERIMENTAL CHARACTERIZATION

An assembly of PJAs corresponding to the modified design shown in Fig. 5-a has been fabricated for comparison with the numerical results and future tests

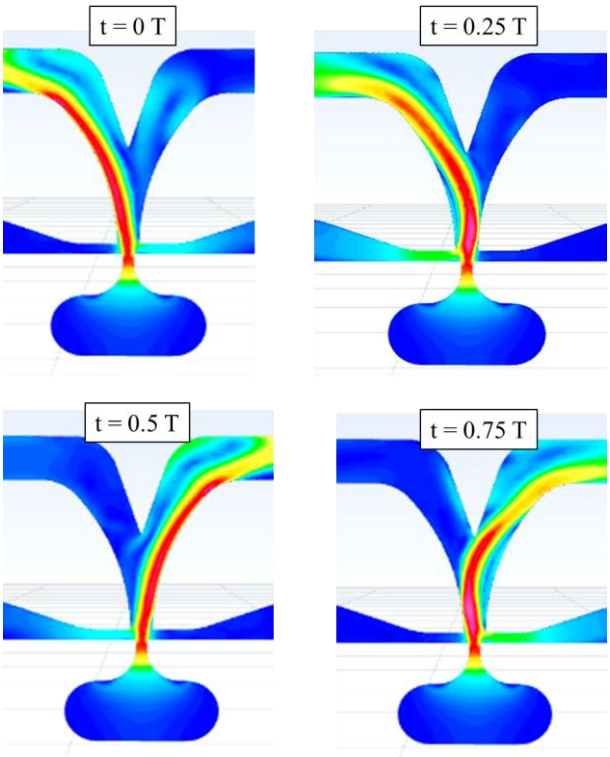

Figure 6: velocity contours in the switching zone at four different times during one period of the oscillation.

on the wind tunnel with the airfoil. The schematic of Fig. 7-a shows the structure of the mounted device consisting of the 3D printed fluidic oscillators, a reservoir to provide the supply pressurized air, a plate separating the fluidic oscillators from the reservoir and a rubber joint. The interface plate separating the reservoir from the oscillators is glued to the 3D printed piece to later screw them to the reservoir with the rubber joint in

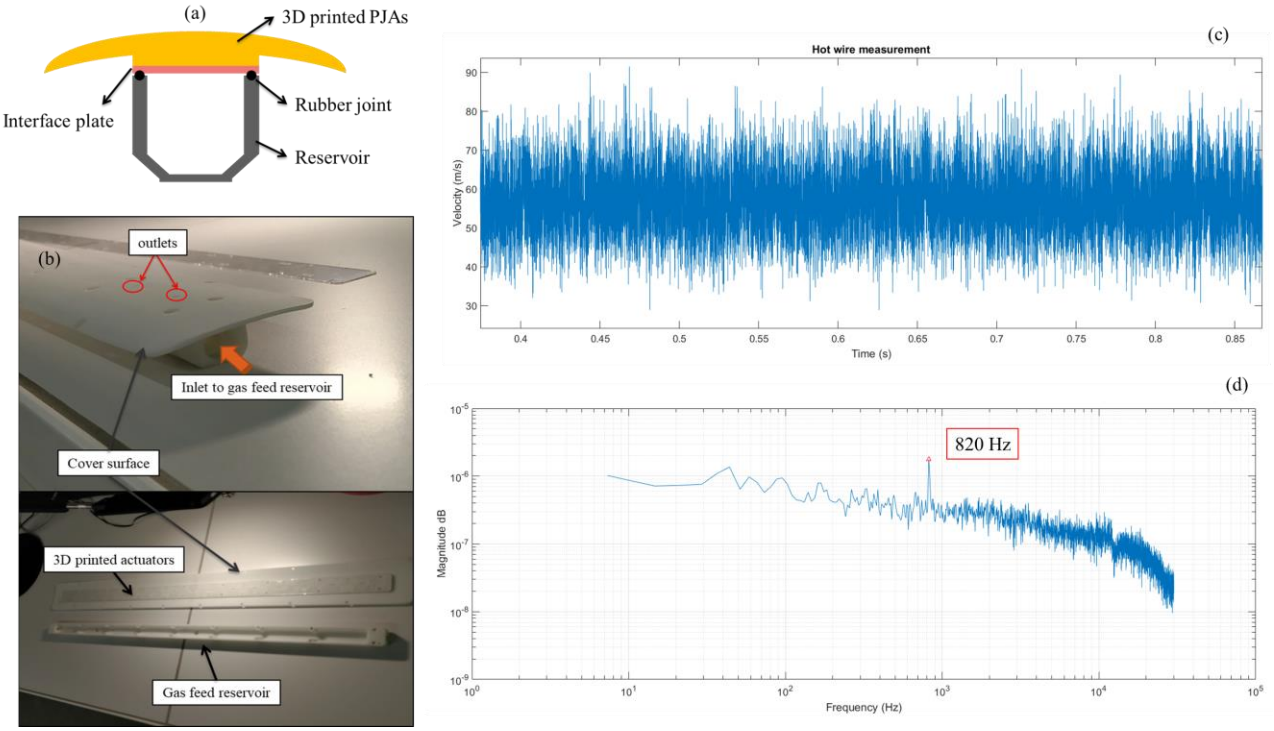

Figure 7: (a) schematic of the PJAs assembly, (b) pictures of the mounting of the actuator, (c) velocity measured with the hot wire anemometry and (d) frequency of the signal acquired using the Welch method.

between the separating plate and the reservoir. Also, the separating plate between the oscillators and the reservoir is pierced in order to let the pressurized air flow from the gas feed reservoir into the fluidic oscillators. Fig. 7-b shows the 3D printed piece and the reservoir before being mounted.

The jet at the outlets has been characterized with hot wire anemometry. A DANTEC probe type 55 hot wire has been used with a frequency of acquisition of 60 kHz. In Fig. 7-c the velocity measured at the outlet of the PJAs is shown, with a range of the velocity measured at the outlet of V_{out} =28.4-93.9 m/s. Compared to the velocity range obtained in the simulation, the measured values are 25% to 36% lower. This can be explained by the fact that the hot wire is not positioned exactly at the outlet, but at a certain distance (less than 5 millimeters) from the outlet section. Regarding the oscillatory frequency, in Fig. 7-c the Welch method is applied to the signal acquired by the hot wire to extract the frequency of oscillation at the outlet. The frequency extracted from the measurement is f =820 Hz, which is almost identical to the frequency obtained in the simulations of 817 Hz, but slightly lower than the theoretical frequency of 850 Hz.

7. CONCLUSIONS

A numerical investigation has been performed in order to design a series of synchronized PJAs to control the flow over a scaled NACA-4412 airfoil. Realistic constraints related to the implementation of the PJAs in the airfoil as well as the fabrication and a targeted performance based on the optimal operation extracted from previous works have been considered. An initial design based on previous works was investigated, however, due to the modifications included to adjust the oscillators to the constraints; the switching of the internal jet between branches was not accomplished. This is mainly due to the high resistance to the flow in the feedback loop derived from the small cross section and high complexity. Therefore, a modified design is proposed in which the cross section of the feedback loop is increased and the resistance to the flow due to the feedback loop complexity is reduced. Additionally, the switching zone is modified in order to induce more easily the Coanda effect and attach the internal jet to the branch walls. A prototype has been fabricated with the geometry of the modified design and characterized with hot wire anemometry. The comparison between the numerical investigation and the experimental measurements shows a good agreement in terms of the oscillatory frequency, while the velocity measured is lower than the simulated one. This is due to the hot wire not being exactly positioned at the outlet, but at a few millimeters from the outlet.

Following the work presented, the next steps are the implementation of the prototype in the NACA-4412 airfoil to characterize the performance of the active flow

control with the PJAs in the wind tunnel of the PRISME Laboratory. Additionally, new iterations further optimizing the designs shown in this work are intended following the first wind tunnel tests.

8. ACKNOWLEDGEMENTS

This project has received funding from the Clean Sky 2 Joint Undertaking (JU) under grant agreement No 887010. The JU receives support from the European Union's Horizon 2020 research and innovation programme and the CleanSky 2 JU members other than the Union.

9. REFERENCES

[1] Simpson, R. L. (1989). Turbulent boundary-layer separation. *Annual Review of Fluid Mechanics*, *21*(1), 205-232.

[2] Seifert, A., Darabi, A., Wyganski, I. (1996). Delay of airfoil stall by periodic excitation. *Journal of aircraft*, 33(4), 691-698.

[3] Cattafesta III, L. N., Sheplak, M. (2011). Actuators for active flow control. *Annual Review of Fluid Mechanics* Vol. 43, 2011, pp. 247-272.

[4] Passagia, P-Y., López Quesada, G., Loyer, S., Baldas, L., Robinet, J-C., Stefes, B., Mazellier, N. (2022). Wind-tunnel experiments and separation control of a NACA4412 with 25º sweep at high Reynolds numbers. *AIAA SciTech 2022 Forum.*

[5] Seifert, A., Pack, L. G. (2002). Active Flow Separation Control on Wall-Mounted Hump at High Reynolds Numbers. *AIAA Journal* Vol. 40, No. 7, pp. 1363-1372.

[6] Luedke, J., Graziosi, P., Kirtley, K., Cerretelli, C. (2005). Characterization of Steady Blowing for Flow Control in a Hump Diffuser. *AIAA Journal* Vol. 43, No. 8, pp. 1644-1652.

[7] Greenblatt, D., Paschal, K. B., Chung-Sheng, Y., Harris, J. (2006). Experimental Investigation of Separation Control Part 2: Zero Mass-Flux Oscillatory Blowing. *AIAA Journal* Vol. 44, No. 12, pp. 2831-2845.

[8] Cerretelli, C., Kirtley, K. (2009). Boundary Layer Separation Control With Fluidic Oscillators. *Journal of Turbomachinery* Vol. 131, No. 4, pp. 041001-041001.

[9] Joseph, P., Bortolus, D., Grasso, F. (2014). Flow control on a 3D backward facing ramp by pulsed jets. *Comptes Rendus Mécanique* Vol. 342, No. 6–7, 2014, pp. 376-381.

[10] Wang S, Batikh A, Baldas L, Kourta A, Mazellier N, Colin S, Orieux S (2019) On the modelling of the switching mechanisms of a Coanda fluidic oscillator. *Sensors and Actuators: A. Physical*, 299, p.111618.